Bypassing Cowling's Theorem in Axisymmetric Fluid Dynamos

Christophe Gissinger, Emmanuel Dormy, Stéphan Fauve

Bypassing Cowling's Theorem in Axisymmetric Fluid Dynamos

Christophe Gissinger,[1] Emmanuel Dormy,[2] and Stephan Fauve[1]

[1]*Laboratoire de Physique Statistique de l'Ecole Normale Supérieure, CNRS UMR 8550, 24 Rue Lhomond, 75231 Paris Cedex 05, France*

[2]*MAG (IPGP/ENS), CNRS UMR 7154, LRA, Ecole Normale Supérieure, 24 Rue Lhomond, 75231 Paris Cedex 05, France*

(Received 9 May 2008; published 1 October 2008)

We present a numerical study of the magnetic field generated by an axisymmetrically forced flow in a spherical domain. We show that, even in the absence of nonaxisymmetric velocity fluctuations, a mean magnetic field with a dominant axisymmetric dipolar component can be generated via a secondary bifurcation from an equatorial dipole. We understand the dynamical behaviors that result from the interaction of equatorial and axial dipolar modes using simple model equations for their amplitudes derived from symmetry arguments.

DOI: 10.1103/PhysRevLett.101.144502 PACS numbers: 47.65.−d, 52.65.Kj, 91.25.Cw

It is strongly believed that magnetic fields of planets and stars are generated by dynamo action, i.e., self-generation of a magnetic field by the flow of an electrically conducting fluid [1]. Planets and stars being rapidly rotating, axisymmetric flows about the axis of rotation have been considered in order to work out simple dynamo models [2]. A major setback of the subject followed the discovery of Cowling's theorem, which stated that a purely axisymmetric magnetic field cannot be maintained by dynamo action [3]. However, it has been shown that magnetic fields with a dominant axisymmetric mean part can be generated when nonaxisymmetric helical fluctuations are superimposed to a mean axisymmetric flow [4]. This has been recently observed: a turbulent swirling von Kármán flow (VKS) driven by two counterrotating coaxial impellers in a cylindrical container, self-generated a magnetic field with a dipole mean component along the axis of rotation [5]. This has been ascribed to an alpha effect due to the helical nature of the radially ejected flow along the two impellers [6].

In this Letter, we show that there exists another mechanism for bypassing the constraint imposed by Cowling's theorem, without the help of nonaxisymmetric turbulent fluctuations. The mechanism is as follows: the primary dynamo bifurcation breaks axisymmetry in agreement with Cowling's theorem. Then, the Lorentz force generates a nonaxisymmetric flow component which can drive an axisymmetric magnetic field through a secondary bifurcation. We show that direct numerical simulations confirm this scenario and that the two successive bifurcation thresholds can be very close in some flow configurations. The existence of two competing instability modes, the axial and equatorial dipoles, can lead to complex dynamical behaviors. Using symmetry arguments, we write equations for the amplitude of these modes that are coupled through the nonaxisymmetric velocity component. We show that the observed bifurcation structure and the resulting dynamics can be understood in the framework of this simple model.

We first numerically integrate the MHD equations in a spherical geometry for the solenoidal velocity $\mathbf{v}$ and magnetic $\mathbf{B}$ fields,

$$\frac{\partial \mathbf{v}}{\partial t} + (\mathbf{v}\cdot\boldsymbol{\nabla})\mathbf{v} = -\boldsymbol{\nabla}\pi + \nu\Delta\mathbf{v} + \mathbf{f} + \frac{1}{\mu_0\rho}(\mathbf{B}\cdot\boldsymbol{\nabla})\mathbf{B}, \quad (1)$$

$$\frac{\partial \mathbf{B}}{\partial t} = \boldsymbol{\nabla}\times(\mathbf{v}\times\mathbf{B}) + \frac{1}{\mu_0\sigma}\Delta\mathbf{B}. \quad (2)$$

In the above equations, ρ is the density, ν is the kinematic viscosity, μ_0 is the magnetic permeability, and σ is the electrical conductivity. The forcing is $\mathbf{f} = f_0\mathbf{F}$, where $F_\phi = s^2\sin(\pi s b)$, $F_z = \varepsilon\sin(\pi s c)$, for $z > 0$, using polar coordinates $(s,\ \phi,\ z)$ (normalized by the radius of the sphere a) and opposite for $z < 0$. F_ϕ generates counterrotating flows in each hemisphere, while F_z enforces a strong poloidal circulation. The forcing is only applied in the region $0.25a < |z| < 0.65a$, $s < s_0$. In the simulations presented here, $s_0 = 0.4$, $b^{-1} = 2s_0$, and $c^{-1} = s_0$. This forcing has previously been introduced to model the mechanical forcing due to coaxial rotating impellers used in the Madison experiment [7]. Although performed in a spherical geometry, this experiment involves a mean flow with a similar topology to that of the VKS experiment. Such flows correspond to $s_2 + t_2$ flows in the Dudley and James classification [2], i.e., two poloidal eddies with inward flow in the midplane, together with two counterrotating toroidal eddies. We solve the above system of equations using the PARODY numerical code [8], originally developed in the context of the geodynamo (spherical shell). We have modified the code to make it suitable for a full sphere. The maximum resolution used here is 500 points in the radial direction, and a spherical harmonic decomposition truncated at $l,\ m < 64$. We use the same dimensionless numbers as in [7], the magnetic Reynolds number $\mathrm{Rm} = \mu_0\sigma a\max(|\mathbf{v}|)$, and the magnetic Prandtl number $\mathrm{Pm} = \nu\mu_0\sigma$. The kinetic Reynolds number is then $\mathrm{Re} = \mathrm{Rm}/\mathrm{Pm}$.

The dynamo threshold Rm_c is displayed as a function of Re in Fig. 1(a). Negative Re corresponds to a flow that is reversed compared to the VKS configuration, i.e., directed

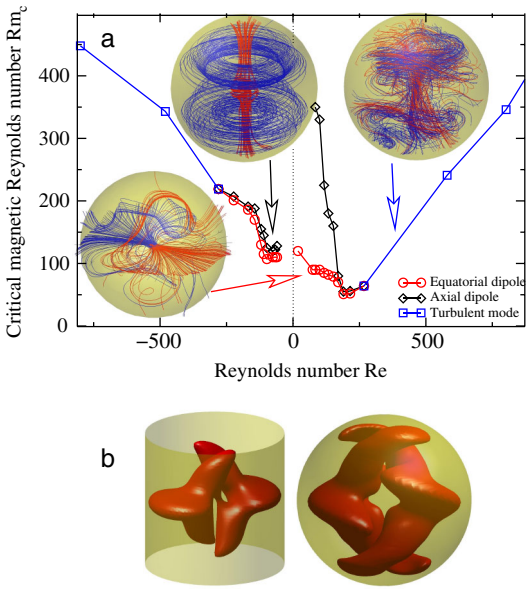

FIG. 1 (color online). (a) Stability curves $\mathrm{Rm}_c = f(\mathrm{Re})$ obtained with direct numerical simulations. In red (or gray): onset of the $m = 1$ (equatorial dipole) dynamo mode; in black: nonlinear threshold of the $m = 0$ (axisymmetric) mode; in blue (or dark gray), the turbulent mode emerging from velocity fluctuations. The corresponding magnetic structures are represented using magnetic field lines. The top right inset, involving a very fluctuating magnetic field, has here been averaged over two magnetic diffusion time. (b) Comparison of the magnetic field (isovalue of the magnetic energy) generated by an axisymmetric $s2 + t2$ flow in a cylinder [11] or a sphere.

from the impellers to the center of the flow volume along the axis and radially outward in the midplane. This corresponds to reversing the sign of the component F_z of the forcing term in the simulations. For small enough Re, the flow is laminar and axisymmetric. A magnetic field with a dominant equatorial dipole mode $m = 1$ is generated first [red (or gray) curve and left inset of Fig. 1(a)]. It breaks axisymmetry as expected from Cowling's theorem. This dynamo mode is similar to that obtained in cylindrical geometry, as illustrated in Fig. 1(b).

For $|\mathrm{Re}|$ larger than about 300, the flow becomes turbulent and the equatorial dipole is then replaced by a dominant axisymmetric mode $m = 0$. Its threshold increases with $|\mathrm{Re}|$ in the parameter range of the simulations [blue (or dark gray) curve and right inset of Fig. 1(a)]. These results are in agreement with [7]. It is remarkable that the axial dipole observed in the VKS experiment and ascribed to nonaxisymmetric fluctuations [6] can also be obtained in the present simulations even though the level of fluctuations is much smaller (the parameter range realized in the experiment being, by far, out of reach of present computer models).

In addition, an axisymmetric magnetic field can also be generated at very low Re through a secondary bifurcation from the equatorial dipole when Rm is increased [black curves and top left inset of Fig. 1(a)]. The bifurcation diagram of Fig. 2 helps to understand the mechanism by which this axisymmetric magnetic field is generated. One can observe that the equatorial dipole first bifurcates supercritically for $\mathrm{Rm} = 88$ when $\mathrm{Re} = 122$. The backreaction of the Lorentz force is twofold. First, it inhibits the axisymmetric velocity field, which decreases [orange (or light gray) curve in Fig. 2]. Second, and more importantly, it drives a nonaxisymmetric $m = 2$ velocity mode [blue (or dark gray) curve in Fig. 2]. Once the intensity of this flow becomes strong enough, it yields a secondary bifurcation of the axisymmetric $m = 0$ field mode. This is achieved for $\mathrm{Rm} = 205$ (black curve in Fig. 2). The amplitude of the equatorial dipole decreases immediately after this secondary bifurcation. We observe that the $m = 0$ mode vanishes at higher Rm and then grows again above $\mathrm{Rm} = 425$. Although the amplitude of the equatorial and axial modes behave in a complex manner as Rm is increased, we observe that they are anticorrelated, thus showing that they inhibit each other through the nonlinear couplings.

For $\mathrm{Re} < 0$, Fig. 1(a) shows that the primary and secondary bifurcations occur in a much narrower range of R_m. The equatorial dipole mode is then close to marginal stability when the axial one bifurcates, and their nonlinear interactions lead to complex time dependent dynamics close to threshold as displayed in Fig. 3. The equatorial mode [red (or gray) curve] is generated first and saturates, but it drives the axial mode (black curve) through the nonaxisymmetric part of the velocity field. The axial dipole then inhibits the equatorial one that decays almost to zero. As a result, the flow is no longer driven away from axisymmetry by the Lorentz force. The axial dipole thus decays and the process repeats roughly periodically. We observe that during one part of the cycle, the magnetic field is almost axisymmetric. It involves a strong azimuthal field together with a large vertical component near the axis of

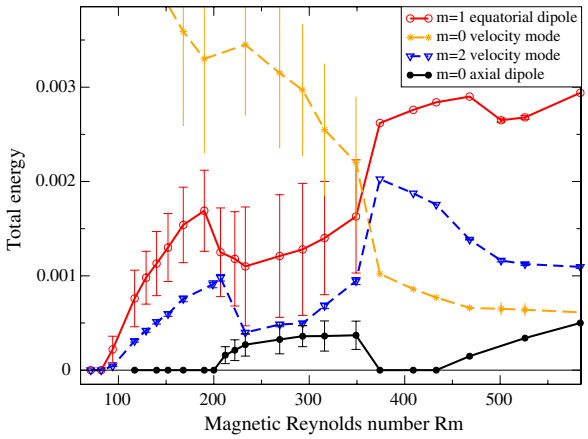

FIG. 2 (color online). Bifurcation diagram of magnetic modes varying Rm with fixed $\mathrm{Re} = 122$. Error bars indicate the amplitude of oscillations. All other magnetic modes are very small compared to these.

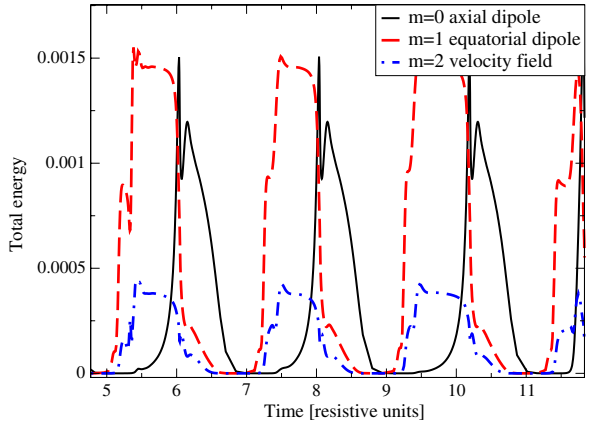

FIG. 3 (color online). Time recordings of the total energy of the equatorial and axial dipolar modes, and of the $m = 2$ velocity mode for Re $= -76$ and Rm $= 170$.

rotation, i.e., an axial dipole [see the left inset of Fig. 1(a)]. These relaxation oscillations, present only in the Re < 0 case, occur slightly above the threshold of the secondary bifurcation of the $m = 0$ mode. Their period first decreases when Rm is increased, but then increases showing a divergence when the relaxation oscillations bifurcate to a stationary regime, as displayed in Fig. 4. Above this transition, we observe bistability with the coexistence of two solutions: a nearly equatorial dipole, with a strong equatorial component and a weak axial one (labeled M_1 in Fig. 4) and a nearly axial dipole (labeled M_2).

We will show next that this competition between equatorial and axial modes, and the resulting dynamics, can be understood using a simple model for the amplitudes of the relevant modes. We thus write

$$\mathbf{B}(\mathbf{r}, t) = A(t)\mathbf{D}_{\mathrm{eq}}(\mathbf{r}) + \mathrm{c.c.} + B(t)\mathbf{D}_{ax}(\mathbf{r}) + \cdots, \quad (3)$$

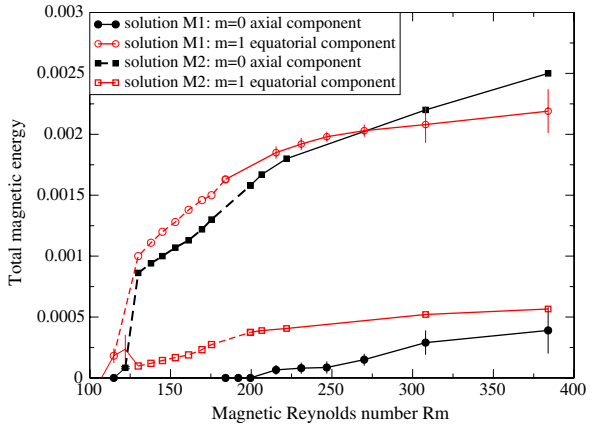

FIG. 4 (color online). Bifurcation diagram of magnetic modes varying Rm at fixed Re $= -76$. Error bars indicate the amplitude of oscillations. Dashed lines correspond to the maximum values of the modes in the relaxation regime. All other magnetic modes are very weak compared to these ones.

where $\mathbf{D}_{\mathrm{eq}}(\mathbf{r})$ [respectively, $\mathbf{D}_{ax}(\mathbf{r})$] is the eigenmode related to the equatorial (respectively, axial) dipole. A is a complex amplitude, its phase describes the angle of the dipole in the equatorial plane and c.c. stands for the complex conjugate of the previous expression. B is a real amplitude. As said above, the equatorial dipole ($m = 1$) generates a nonaxisymmetric flow through the action of the Lorentz force. The later depends quadratically on the magnetic field. This nonaxisymmetric velocity mode of complex amplitude $V(t)$ thus corresponds to $m = 2$. Using symmetry arguments, i.e., rotational invariance about the z axis which implies the invariance of the amplitude equations under $A \to A\exp i\chi$, $V \to V\exp 2i\chi$, and the $\mathbf{B} \to -\mathbf{B}$ symmetry, we get up to the third order

$$\dot{A} = \mu A - V\bar{A} - \alpha_1|A|^2A - \alpha_2|V|^2A - \alpha_3B^2A, \quad (4)$$

$$\dot{V} = -\nu V + A^2 - \beta_1|A|^2V - \beta_2|V|^2V - \beta_3B^2V, \quad (5)$$

$$\dot{B} = -\lambda B - \gamma_1|A|^2B + \gamma_2|V|^2B - \gamma_3B^3. \quad (6)$$

μ is proportional to the distance to the dynamo threshold. Clearly $\nu > 0$, since the flow is axisymmetric below threshold. The coefficients of the quadratic terms can be scaled by an appropriate choice of the amplitudes. The term A^2 represents the forcing of the nonaxisymmetric flow by the Lorentz force related to the equatorial dipole. $V\bar{A}$ means that rotational invariance for the equatorial dipole is broken as soon as a nonaxisymmetric flow is generated. We have fixed its sign so that the bifurcation of the equatorial dipole remains supercritical $\forall\, \alpha_1 \geq 0$. The equations for A and V (with $B = 0$) are the normal form of a 1:2 resonance [9] and have been studied in details in other contexts. In particular, it is known that this system can undergo a secondary bifurcation for which the phase of A begins to drift at constant velocity when μ reaches a value such that $|A|^2 = 2|V|^2$. This corresponds here to a dipole, rotating at constant rate in the equatorial plane. Consider now the equation for the amplitude B of the axial magnetic field. Taking $\lambda > 0$ and $\gamma_3 > 0$ ensures that it cannot be generated alone, in agreement with Cowling's theorem. The term $|V|^2B$ describes the possible amplification of B from the nonaxisymmetric velocity field provided that $\gamma_2 > 0$. Although the system of amplitude Eqs. (4)–(6) cannot be derived asymptotically from (1) and (2), it reproduces the phenomenology observed with the direct simulations for both signs of Re: when μ is increased, we either obtain relaxation oscillations as for Re < 0 (parameters of Fig. 5) or a secondary bifurcation of the axial field as for Re > 0 (same parameters with $\gamma_2 = 1$). The relaxation oscillations are displayed in Fig. 5 (left). The model helps to understand the qualitative features observed in the direct simulation: for small values of μ, it involves a solution corresponding to an equatorial dipole (A_0, V_0, $B = 0$). When μ is increased, the equatorial dipole first undergoes a pitchfork bifurcation to a mixed mode $M = (A_1, V_1, B_1)$

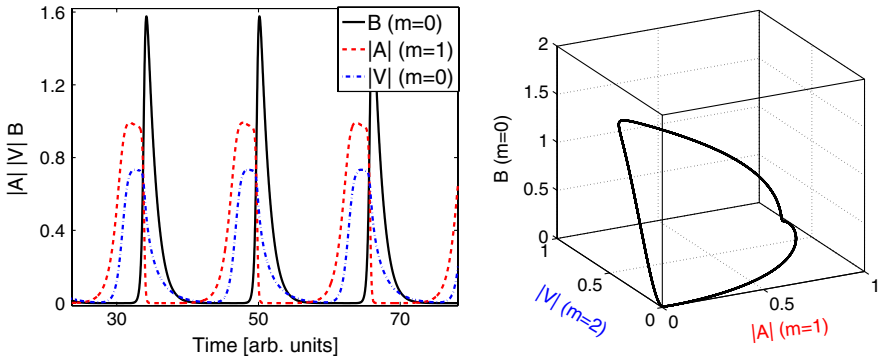

FIG. 5 (color online). Numerical integration of the amplitude equations (4)–(6). Left: time recordings of the amplitudes of the equatorial and axial magnetic modes interacting through the nonaxisymmetric velocity mode ($\mu = 1$, $\alpha_1 = 0.3$, $\alpha_3 = 4$, $\nu = 0.5$, $\beta_2 = 1.5$, $\lambda = 1$, $\gamma_2 = 10$, $\gamma_3 = 0.5$, all other coefficients being zero). Right: relaxation cycle in phase space.

involving a nonzero axial field. M then bifurcates to a limit cycle that displays a relaxation behavior, slowing down in the vicinity of M and O, as its amplitude increases (see Fig. 5).

Let us note that this relaxation behavior extends to a large domain of the parameter space, in particular, it is very robust to a modification of the linear coefficients μ, ν, λ. However the model does not describe the transition from the limit cycle to the bistable stationary solutions $M1$ and $M2$ observed at larger values of Rm in the full numerics (see Fig. 5).

In sodium flows driven by an axisymmetric forcing, such as the ones used in the VKS [5], Madison and Maryland experiments [10], one expects a possible competition between equatorial and axial dynamo modes. Indeed, the mean flow, if it were acting alone, would generate an equatorial dipole in agreement with Cowling's theorem. Our direct simulations show that a fairly small amount of nonaxisymmetric fluctuations (compared to the experiments) is enough to drive an axial ($m = 0$) dipole as observed in the VKS experiment for the mean magnetic field. In addition, we show here that even without turbulent fluctuations, the nonaxisymmetric flow driven by the Lorentz force related to the equatorial dipole, can generate the axial one through a secondary bifurcation. The equatorial dipole can easily rotate in the equatorial plane, thus averaging to zero. The axial dipole then becomes the dominant part of the mean magnetic field.

It is striking that this mechanism that generates an axial dipole occurs much closer to the dynamo threshold when we go from the $\mathrm{Re} > 0$ to the $\mathrm{Re} < 0$ flow configuration, thus when the product of the helicity times the differential rotation is changed to its opposite value. For $\mathrm{Re} < 0$, the shear layer in the midplane becomes favorable to an α-ω dynamo as soon as the axisymmetry of the flow is broken. For $\mathrm{Re} > 0$, the flow near the impellers can play a similar role but the effect is weaker. This opens interesting perspectives for flows that can be used for future dynamo experiments: an α-ω effect driven by the strong vortices present in the shear layer close to the midplane can be favored by the $\mathrm{Re} < 0$ configuration. To wit, one can use either the optimized setup described in [6] or propellers with the appropriate pitch in the VKS or Madison experiments.

A competition between the equatorial and axial dipolar modes could also account for secular variations of Earth's magnetic field. It would be interesting to check whether some features can be described with a low dimensional model similar to the one used in this study.

Computations were performed at CEMAG and IDRIS.

[1] H. K. Moffatt, *Magnetic Field Generation in Electrically Conducting Fluids* (Cambridge University Press, Cambridge, 1978); *Mathematical Aspects of Natural Dynamos*, edited by E. Dormy and A. M. Soward (CRC Press, Boca Raton, 2007).
[2] M. L. Dudley and R. W. James, Proc. R. Soc. A **425**, 407 (1989), and references therein.
[3] T. G. Cowling, Mon. Not. R. Astron. Soc. **94**, 39 (1934).
[4] E. N. Parker, Astrophys. J. **122**, 293 (1955); S. I. Braginsky, Sov. Phys. JETP **20**, 726 (1964); Sov. Phys. JETP **20**, 1462 (1965); F. Krause and K.-H. Rädler, *Mean Field Magnetohydrodynamics and Dynamo Theory* (Pergamon Press, New York, 1980).
[5] R. Monchaux *et al.*, Phys. Rev. Lett. **98**, 044502 (2007); M. Berhanu *et al.*, Europhys. Lett. **77**, 59001 (2007).
[6] F. Pétrélis, N. Mordant, and S. Fauve, Geophys. Astrophys. Fluid Dyn. **101**, 289 (2007).
[7] R. A. Bayliss *et al.*, Phys. Rev. E **75**, 026303 (2007).
[8] E. Dormy, P. Cardin, and D. Jault, Earth Planet. Sci. Lett. **160**, 15 (1998) and later collaborative developments.
[9] G. Dangelmayr, Dyn. Stab. Syst. **1**, 159 (1986); D. Armbuster, J. Guckenheimer, and P. Holmes, Physica (Amsterdam) **29D**, 257 (1988); M. R. E. Proctor and C. Jones, J. Fluid Mech. **188**, 301 (1988).
[10] N. L. Peffley, A. B. Cawthorne, and D. P. Lathrop, Phys. Rev. E **61**, 5287 (2000); M. D. Nornberg, E. J. Spence *et al.*, Phys. Rev. Lett. **97**, 044503 (2006).
[11] C. Gissinger *et al.*, Europhys. Lett. **82**, 29001 (2008).